

Visual Feedback Control of Tensegrity Robotic Systems

Haresh Karnan¹, Raman Goyal¹, Manoranjan Majji¹, Robert E. Skelton¹ and Puneet Singla²

Abstract—Feedback control problems pertaining to the control of tensegrity robotic systems are detailed in this paper. The unique problems that arise due to the positivity of the string tensions required to maintain the static stability and desirable stiffness of the structural system are shown to bring about interesting opportunities to optimize for the redundancy in the actuation process. The static stability consideration, coupled with the nonlinear dynamics and the sensor models introduce additional algebraic constraints in implementation of both kinematic and model based dynamic controllers for tensegrity systems. Approaches to develop kinematic and dynamic control techniques are detailed in this paper. A bench top experimental setup consisting of a simple tensegrity system is utilized to demonstrate the efficacy of the output feedback control approach developed in the paper. Near real time image measurements are utilized to drive the output error used in the control scheme.

I. INTRODUCTION

Revolutions in microelectronics, computing, and materials science usher-in a human robot symbiosis long envisioned by technology seers [1], [2], [3] as an imminent and immediate consequence. To this end, human co-robot collaborative work is slated to impact a wide variety of fields, including advanced manufacturing[4], infrastructure advancement[5], [6], precision agriculture[7], [8], disaster relief[9] and healthcare[10]. Although significant effort is currently being expended to bridge the divide between humans and the co-robots working cooperatively, a variety of significant challenges exist to facilitate their seamless interaction, workload planning and task allocation, motion planning, health monitoring, skill assessment and determination of the levels of autonomy.

A key technical challenge in negotiating this divide between humans and co-robots is to quantify the skill level associated with anthropoid mechanisms to facilitate the development of redundant control techniques and approaches to synthesize equivalent mechanisms and models that capture the biomechanics with sufficient fidelity. Although the kinematic models frequently employed (cf. excellent work by Feix et al [11], [12]) are very useful in defining the functionality, biomechanics and isolating singularities associated with the anthropoid limbs, they do not reveal the load dependent[13], [14] characteristics of the physical system. For instance, the facility of a human using chopsticks is an implicit function of the weight distribution of the sticks

involved. This is also reflected in the variations of hand-writing typically noticed when using different media (i.e., pen, stylus and paintbrush). To facilitate a comprehensive evaluation of the gripping action of the anthropoid grasp, a detailed mathematical model of the mechano-physiological system is vital. Recent advances in structural mechanics and control provided a mechanism to derive such physical and mathematical models in terms of tensegrity systems [15].

Tensegrity is a word coined (tension+integrity) in the art/architecture world by Buckminster Fuller. But the engineering/mathematical characterization of this class of structures is very old. In mathematics and engineering, this class is called a pre-stressable structure, composed of compressive and tensile members (if external forces are present, they also play a role in the prestressability conditions). Recent mathematical results by Skelton et al [16] show that the minimal mass structure (subject to a stiffness constraint) is a tensegrity structure, for each of the five fundamental problems in engineering mechanics: (i) structures loaded in compression, (ii) structures loaded in tension, (iii) structures loaded in cantilevered bending, (iv) structures loaded in torsion, (v) structures loaded in simply-supported bending. Building upon observations of Harvard biologist Don Ingber [17], [18] who identifies tensegrity architecture as the “architecture of life”, we exploit the modular nature of tensegrity structures to realize equivalent models for dexterity quantification of the human and robotic gripping actions.

Tensegrity systems have tremendous potential and depending on the design, may offer a large degree of redundancy in terms of number of control inputs and the actuators used to execute the signals. This is amply evident by examining the bio mechanical systems where the tensions in the tendons actuate bones of the structural system. A critical examination of musculoskeletal biomechanics also brings about certain considerations about actuating tensegrity systems. An important consideration is the loss of stiffness owing to the slackness of certain strings. Depending on the structural design, this aspect may be undesirable for the application of interest. If too many strings lose tension in the actuation process, the structure will certainly collapse. The configurations that maintain desirable stiffness of the tensegrity system at a given point of time are said to be stable. In order to facilitate appropriate actuation without loss of stability of the structural system, certain constraints on the tension of the strings need to be maintained during the actuation process. The shape change affected by deploying actuators while maintaining stable configuration is a key control objective in the control of tensegrity systems. In this paper, feedback control methods that accomplish the shape change, while maintaining the

¹H. Karnan, R. Goyal, M. Majji, and R. E. Skelton are with the Department of Aerospace Engineering, Texas A&M University, Texas, USA haresh.miriyala@tamu.edu mmajji@tamu.edu, bobskelton@tamu.edu

²P. Singla is with Mechanical and Aerospace Engineering, University at Buffalo, New York, USA psingla@buffalo.edu

stability constraints are developed. Kinematic controllers that are designed to stabilize the tracking error dynamics are shown to achieve this complex task of manipulation. Experimental demonstration of the output feedback control scheme provides a basis for optimism for more complex model based control architectures for control of tensegrity robots.

The mathematical models of tensegrity systems are first detailed, alluding to the stability constraints imposed by the structural robotic system. This is followed by a discussion on the output feedback controller design that is aimed at deriving control laws that minimize the sensed output errors. Introduction of stability constraints that are function of the state variables in the feedback control design is accomplished by defining additional output errors that are to be minimized by the feedback controller. The technical details associated with the development of a nonlinear control scheme with these stability constraints are detailed in the next section. Details associated with the experimental prototype used to evaluate the ideas developed in the proposed research are outlined in the subsequent section. This is followed by a discussion on the experimental results obtained from the tracking control experiment using the prototype. The remarks on lessons learned conclude the paper.

II. TENSEGRITY SYSTEMS: MATHEMATICAL MODELING

Recent work by Skelton et al., [16] involves the development of a distinct new approach for multibody dynamics, where the vector formalism to describe the center of mass of a system of rods and strings is used, along with the direction of the rods. By subjecting the bar vectors, (denoted by \mathbf{b}_i to represent the physical vector for the i^{th} rod connecting two nodes \mathbf{n}_{2i} and \mathbf{n}_{2i-1}) that represent the directions of the rod in the global coordinate system to the norm constraints, a fairly generic approach to dynamics is developed by Skelton [19], [20]. The equations governing the evolution of the nodal coordinate vectors for the multibody system are shown to be governed by the matrix equation

$$\ddot{N}\mathcal{M} + N\mathcal{K} = W \quad (1)$$

where $\mathcal{M} = \frac{1}{12}C_b^T \hat{m}C_b + C_r^T \hat{m}C_r$ is a mass matrix and $\mathcal{K} = C_s^T \hat{\gamma}C_s - C_b^T \hat{\lambda}C_b$ is a matrix, that includes the forces exerted by the strings and the constraint force to maintain the normality of the bar vector. $\hat{\lambda} = \frac{1}{2}\hat{l}^{-2}B^T (NC_s^T \hat{\gamma}C_s - W)C_b^T - \frac{1}{12}\hat{l}^{-2}\hat{m}\dot{B}^T \dot{B}$ and $\hat{\gamma}$ represents the force density (force in the member/length of the member) in the bars and strings respectively. N is the matrix of the nodal coordinates describing the configuration of the tensegrity system, W is the matrix of external forces applied on the system and \hat{l} denotes the diagonal matrix of the lengths of the rods in the assembly. The floor operator $[\cdot]$ denotes the diagonalization of the enclosed matrix, \hat{m} denotes a diagonal matrix of the masses of the links, C_s is the connectivity matrix associated with the strings, C_b denotes the connectivity matrix associated with the bars and $C_r = \frac{1}{2}[[C_b]]$ where $[\cdot]$ operator only takes the positive values in the matrix. More details of the approach

are provided in the papers [19], [20] and the book by Skelton [16]. Constraints associated with the nodal connectivity when k rods are connected are incorporated by a set of linear constraint equations written as $NP = D$, where P and D are the constant matrices that specify nodal connectivity. Since the formulation is entirely carried out in a global coordinate system, the connectivity matrix remains constant, facilitating effective and efficient numerical integration process. This leads to a system of matrix differential algebraic equations (DAEs)

$$\ddot{N}\mathcal{M} + N\mathcal{K} = W + \Omega P^T \quad (2)$$

where Ω represents the Lagrange multiplier that needs to be solved using algebraic equations.

As outlined in the introduction, stability considerations associated with the stiffness of the tensegrity system form an important set of constraints to be maintained while traversing through the shape changes stipulated as a part of the objectives of the control system design. It is therefore imperative for the control engineers to ensure there is sufficient redundancy to achieve this. There are several approaches to introduce stiffness in the structure to be imposed during the shape change process. It may be accomplished using pre-stress conditions on the strings of interest $\gamma_i = k_i \left(1 - \frac{s_{0i}}{s_i}\right)$, where, γ_i is the stress or tension level that is associated with the pre-stress value in the i^{th} string, while s is the true control variable and denotes the actual length of the string and s_0 denotes the rest length of the string. Note that the string tension γ_i is a nonlinear function of the nodal coordinates N . Empirically derived stability considerations and acceptable values of pre-stress may be written as $\Phi(N) = 0$. Note that the stability considerations now impose the satisfaction of $\Phi(N) = 0$ as an additional set of tracking objectives.

III. FEEDBACK CONTROL

With reference to the matrix dynamics of the tensegrity system, i.e., Eq. 1, let us now derive a feedback control system to minimize a tracking error criteria. If Y_T is the set of node points to be traversed by the tensegrity system, the errors incurred by the structural system can be written as

$$E := NR - Y_T \quad (3)$$

where R is a constant matrix that is required for tracking of some particular nodes. This definition allows us to define the error rate as $\dot{E} = \dot{N}R$ and the second derivative of the error is written as $\ddot{E} = \ddot{N}R$. Using equations of motion in the error dynamics, we see that

$$\ddot{E} = (W + \Omega P^T - N\mathcal{K})\mathcal{M}^{-1}R \quad (4)$$

For stabilization of the error dynamics, we stipulate that the error accelerations assume the form

$$\ddot{E} = -EK_p - \dot{E}K_d \quad (5)$$

with the additional stipulation that output feedback gains K_p and K_d are positive definite gain matrices chosen arbitrarily. Note that a much more general feedback control structure

can be achieved by vectorizing the matrix equation. These structures are not discussed here to maintain brevity of the technical developments. To achieve the error dynamics of Eq. 5, we can solve the linear algebra problem, obtained by substituting Eq. 4 in to Eq. 5, written as

$$(W + \Omega P^T - NK) \mathcal{M}^{-1} R = -EK_p - \dot{E}K_d \quad (6)$$

Note that the control law of Eq. 6 is unaware of the stability considerations associated with the prestress of the strings (i.e., $\Phi(N)$). To ensure these considerations, the tracking error state E is augmented with the state constraints Φ , giving rise to a new tracking error state $\tilde{E} = [E \ \Phi]$. Depending on the application of interest, one may implement a first order control scheme, where the closed loop error dynamics is of the form $\dot{\tilde{E}} - A\tilde{E} = 0$, where A is a Hurwitz matrix with all negative eigenvalues. A second order structure can also be used for the output feedback control law. This will have the same form as Eq. 5.

IV. EXPERIMENTAL SETUP

Let us explain the experimental setup for this robot. We start with a benchtop planar model of a D-bar tensegrity structure. Typically this structure consists of 4 compressive members and 2 tensile members. In order to increase the freedom in the motion of the structure, we combined it with 2 more strings to let it move around a pin joint.

Fig.1 shows four bars connected in a diamond shape through four hollow female pin joints, which were 3D printed in ABS, with cylindrical aluminium supports at its centre acting as a compliant mechanism to reduce friction between joints and to provide a path for the free movement of strings. This structure has a total of four strings being actuated, one vertical (S1), one horizontal (S2) and two strings connected to two nodes (S3 and S4) to allow it to move about a pin joint as shown in Fig.3. The material used here is brass and UHMWPE (commonly known as SPECTRA) for bars and strings respectively. The bars measure 6 inches in length, with an outer diameter of 0.25 inches.

All four strings in the setup are passed through a spool of large radius to get the required feed rate and provide frictionless movement for strings. The spools are 3D printed out of PLA. These four strings are directly controlled by four AX-12A dynamixel servo motors attached to the spools. The AX-12A dynamixel servo has the ability to track its speed, temperature, shaft position, voltage, and load. They are controlled using a script written in Python and communicates with the computer via a USB2DYNAMIXEL controller in a daisy chain link.

A USB camera of resolution (720p) is used to sense the node positions of the three nodes (marked green in the Fig. 1). Fig. 2 shows the mounting setup for the camera. To extract the node coordinates from the calibrated image, we first convert the BGR image obtained from the camera to HSV image space and filter out the green components in the image. Then, to get the coordinate positions of nodes, we threshold the grayscale version of the filtered green image to create a mask image and find the contour moments of the black

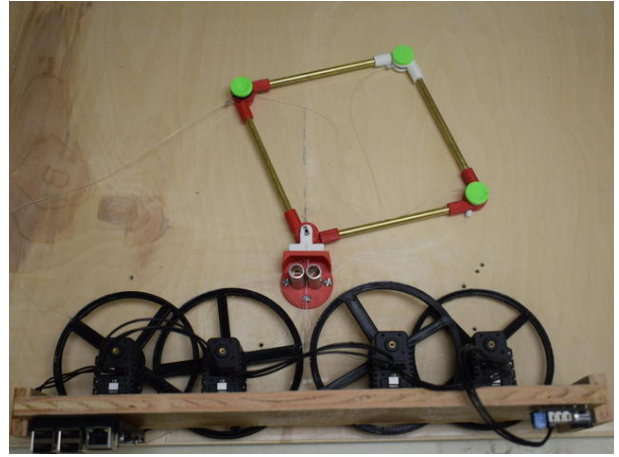


Fig. 1: Experimental Setup

and white mask. Then a simple coordinate transformation gives the coordinates of the nodes with respect to the pinned node as origin. With these obtained nodes, we calculate the different angles needed to capture the kinematics of the Dbar Tensegrity system, which we later feed into to the controller to drive the errors to zero.

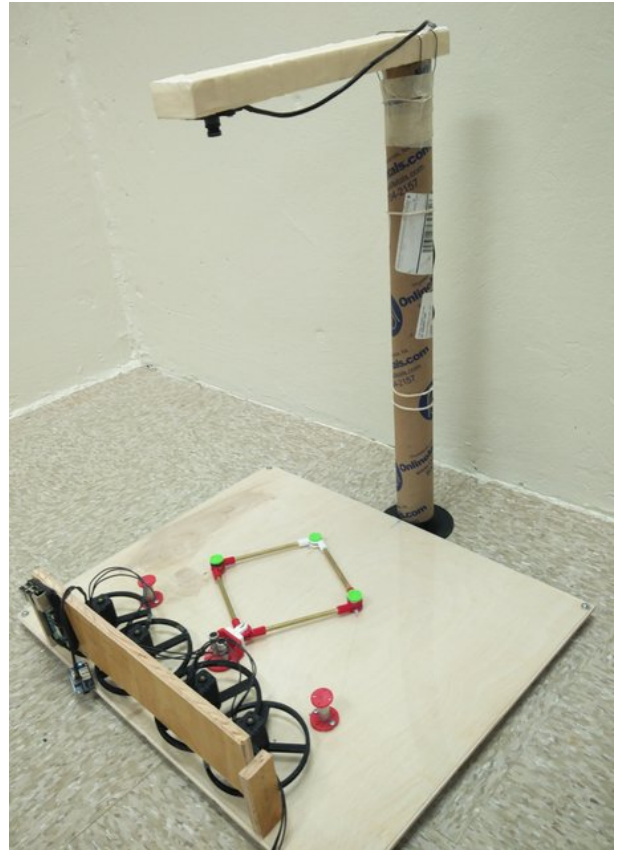


Fig. 2: Camera Mounting

V. RESULTS

The test setup detailed in the previous section is now utilized to demonstrate the efficacy of the feedback con-

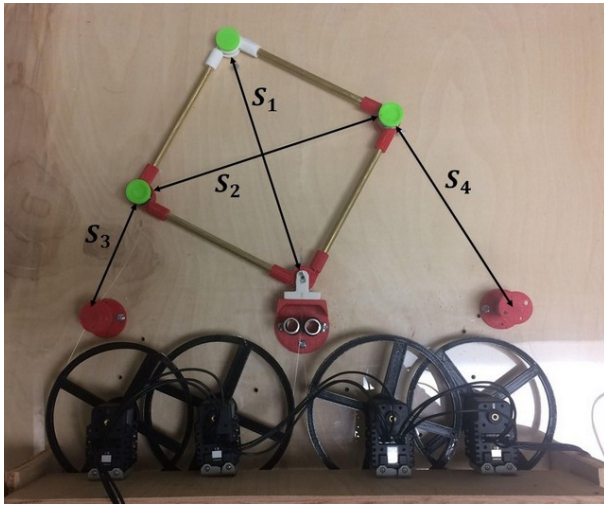


Fig. 3: String Indexing

control methodology explained earlier. The node tracking error discussed in the previous section and its rate are populated using the camera feed directly. Fig. 4 plots the tracking error incurred by the feedback control system when tracking the ellipse prescribed as shown in Fig. 11. The tracks achieved by the D-bar system (in black) when tracking a circular trajectory and a straight line trajectory (magenta) are shown in Figs. 9 and 10 respectively. From the error time histories plotted in Fig. 4, it is clear that during the second half of the tracking error cycle, the errors incurred in the radial and tangential direction are found to increase. The physical reason for this relates to the fact that the tensions incurred by the actuation system to achieve the tracking force the bars to leave the plane. This process introduces fictitious errors in the plane that is shown around 12 seconds in the tangential tracking error plot of Fig. 4. Since the error feedback signal is derived from a projection of the image viewing the robot from an orthographic view, the off-plane deviation is unobservable and hence cannot rectify itself. Future versions of the control loop will modify this setup to minimize the out of plane motion of the 2D mechanism.

The string length time histories assumed by the motors to achieve the tracking error performance associated with the ellipse tracking are shown in Fig. 5 to Fig. 8. These preliminary results offer a basis for optimism about the utility of the feedback control schemes developed in this paper for control of more complex tensegrity systems.

VI. CONCLUSIONS

Feedback control formulations, useful to manipulate tensegrity robots to affect shape changes of certain nodes of the structure are presented. It is shown that augmenting the feedback control errors with the stabilization constraints provides an effective means of achieving control approaches that are sensitive to the stiffness constraint stipulations necessary to maintain the structural stability requirements of the tensegrity structure. An experimental platform comprising

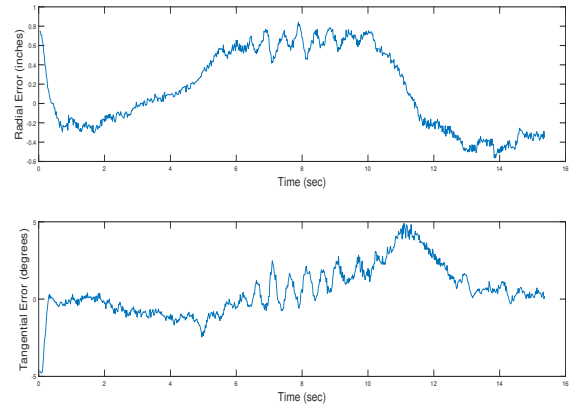


Fig. 4: Time history of Radial and Tangential Errors

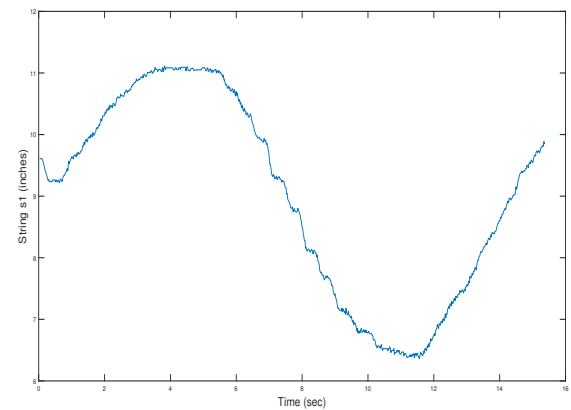


Fig. 5: Time history of length of string S1

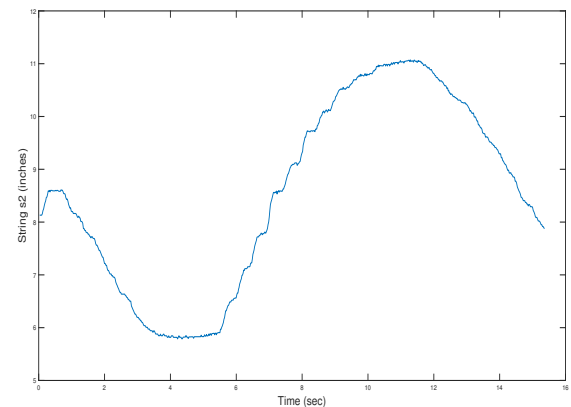


Fig. 6: Time history of length of string S2

of a bench-top planar tensegrity 4bar mechanism (called D-bar) is developed, with a camera system as the sensor system. The feedback control schemes derived in the paper are applied to use the D-bar system to track a few reference trajectories. The tracking errors achieved by the preliminary results demonstrate the utility of the proposed schemes

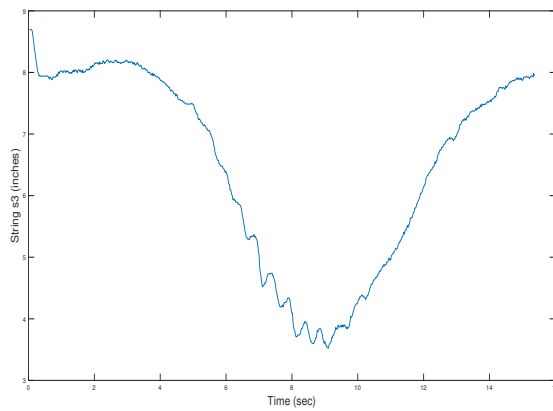


Fig. 7: Time history of length of string S3

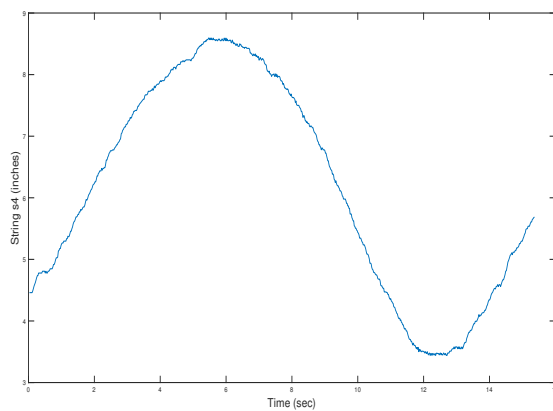


Fig. 8: Time history of length of string S4

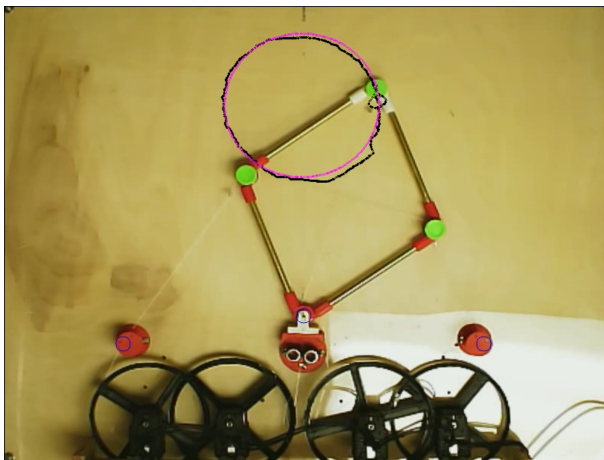


Fig. 9: Circle Tracking

and form a basis of optimism for its application in more complicated structures. Further work is necessary to extend the presented approach to derive model based nonlinear and optimal control laws subjected to state variable inequality constraints.

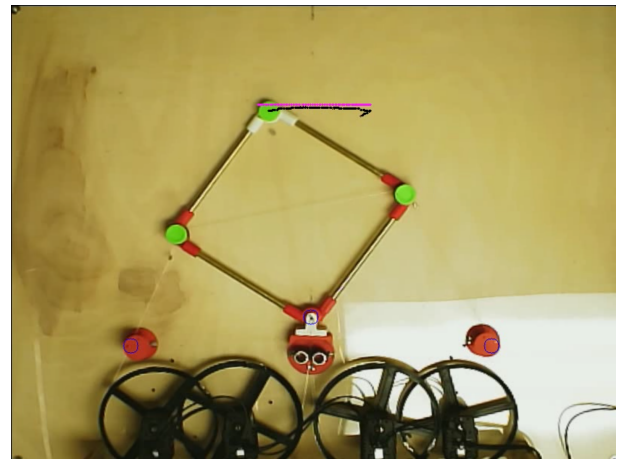


Fig. 10: Line Tracking

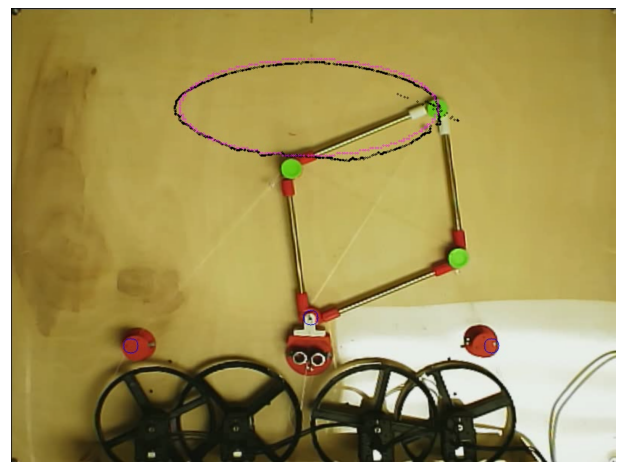


Fig. 11: Ellipse Tracking

REFERENCES

- [1] R. Ambrose, "Nasa technology roadmaps - ta 4: Robotics and autonomous systems," National Aeronautics and Space Administration (NASA), NASA Headquarters, Washington, D.C., Technical Report, July 2015.
- [2] *DARPA Robotics Challenge: Amazing Moments, Lessons Learned and What's Next*, 2015.
- [3] J. P. Holdren and E. Lander, Eds., *Report to the President on Capturing Domestic Competitive Advantage in Advanced Manufacturing*. Executive Office of the President of the United States, July 2012.
- [4] Y. Altintas, *Manufacturing Automation*, 2nd ed. Cambridge University Press, 2012.
- [5] J. Zhang, M. Kaess, and S. Singh, "Real-time depth enhanced monocular odometry," in *Proceedings of the Intelligent Robots and Systems (IROS)*. Chicago, IL: IEEE, 2014.
- [6] C. Doyle and R. Betti, Eds., *Aging Infrastructure: Issues, Research, and Technology*, vol. BIPS 01. U.S. Department of Homeland Security, 2010.
- [7] J. W. Hofstee, L. E. E. M. Spatjens, and H. IJken, "Optimal path planning for field operations," in *Precision Agriculture - 09*, E. J. van Henten, D. Goense, and C. Lokhorst, Eds. Wageningen, the Netherlands: Wageningen Academic Publications, July 2009.
- [8] M. Anderson. (2016) Mit's food computer: The future of urban agriculture?
- [9] R. Murphy, "International cooperation in deploying robots for disasters: Lessons for the future from the great east japan earthquake," *Journal of the Robotics Society of Japan*, vol. 32, no. 2, pp. 104–109, 2014.

- [10] T. Tamura, S. Yonemitsu, A. Itoh, and K. Nakajima, "Is an entertainment robot useful in the care of elderly people with severe dementia?" *Journal of Gerontology: MEDICAL SCIENCES*, vol. 59A, no. 1, pp. 83–85, 2004.
- [11] T. Feix, I. M. Bullock, and A. M. Dollar, "Analysis of human grasping behavior: Object characteristics and grasp type," *IEEE Transactions on Haptics*, vol. 7, no. 3, pp. 311–323, 2014.
- [12] T. Feix, J. Romero, H.-B. Schmiedmayer, A. M. Dollar, and D. Kragic, "The grasp taxonomy of human grasp types," *IEEE Transactions on Human-Machine Systems*, In Press.
- [13] D. M. Wolpert, Z. Ghahramani, and M. I. Jordan, "An internal model for sensorimotor integration," *Science*, vol. 269, no. 5232, p. 1880, 1995.
- [14] C. M. Harris and D. M. Wolpert, "Signal dependent noise determines motor planning," *Nature*, vol. 394, no. 6695, pp. 780–784, 1998.
- [15] R. L. Swanson, "Biotensegrity: A unifying theory of biological architecture with applications to osteopathic practice, education and research - a review and analysis," *The Journal of American Osteopathic Association*, vol. 113, no. 1, pp. 34–52, 2013.
- [16] R. E. Skelton and M. C. deOliveira, *Tensegrity Systems*. Springer, 2009, vol. 1.
- [17] C. S. Chen and D. E. Ingber, "Tensegrity and mechanoregulation: From skeleton to cyto skeleton," *Osteoarthritis Cartilage*, vol. 7, no. 1, pp. 81–94, 1999.
- [18] D. E. Ingber, "Cellular tensegrity: Defining new rules of biological design that govern the cytoskeleton," *Journal of Cellular Science*, vol. 104, no. 3, pp. 613–647, 1993.
- [19] J. Cheong, R. E. Skelton, and Y. Cho, "A numerical algorithm for tensegrity dynamics with non-minimal coordinates," *Mechanics Research Communications*, vol. 58, pp. 46–52, 2014.
- [20] J. Cheong and R. E. Skelton, "Nonminimal dynamics of general class k tensegrity systems," *International Journal of Structural Stability and Dynamics*, vol. 15, no. 2, pp. 1 450 042–(1–22), 2015.